Preparation of a SERS substrate and its sample-loading method for point-of-use application

Nanotechnology **20** (2009) 405604 (9pp) doi:10.1088/0957-4484/20/40/405604

Preparation of a SERS substrate and its sample-loading method for point-of-use application

C Fang, A Agarwal, H Ji, W Y Karen and L Yobas

Institute of Microelectronics, A*STAR (Agency for Science, Technology and Research), 11 Science Park Road, Singapore Science Park II, Singapore

E-mail: fangc@ime.a-star.edu.sg

Received 3 July 2009
Published 8 September 2009
Online at stacks.iop.org/Nano/20/405604

Abstract

A simple approach was demonstrated to prepare a silver (Ag) nanoparticle (NP) assembly as a SERS substrate. Just by dipping a flat silicon (Si) wafer into an aqueous deposition solution of hydrogen fluoride (HF) + silver nitrate ($AgNO_3$), a monolayer of Ag NPs was uniformly deposited onto the Si wafer surface. In order to load the to-be-detected sample onto the as-prepared SERS substrate, three methods have been individually tested, (i) by incubating the SERS substrate in the sample solution, (ii) by dropping and drying a small volume of the sample solution (1–2 μl) onto the SERS substrate surface, or (iii) by directly introducing the sample into the deposition solution. The last approach was also employed to metalize a Si nanowire (NW). Due to the NW's highly curved surface, the Ag NPs self-assembled and aggregated along the NW with a close interdistance. The aggregated Ag NPs on the NW surface can also be used as a SERS substrate. The demonstrated approach holds the promise to prepare a fresh SERS substrate at the point-of-use with the sample already loaded to promptly collect the SERS signal for the field application.

(Some figures in this article are in colour only in the electronic version)

1. Introduction

The discovery of surface-enhanced Raman scattering (SERS) triggered a new research topic in the last decades due to its extremely high sensitivity, which exhibits the capability for single molecule detection [1–3]. The high sensitivity originates from the strong enhancement occurring on the substrate surface, including electromagnetic and chemical contributions. Usually the former, which is related to the nanostructure on the substrate surface, dominates the enhancement interaction. The commonly used SERS substrates include metal nanoparticle (NP) assemblies, electrochemically roughened metal surfaces and nanofabricated substrates etc [2, 4]. Compared to the random distribution of nanostructure on the metal NP assembly and on the roughened metal surface, the nanofabricated SERS substrate is developed to intentionally arrange the nanostructure. The sensitivity of the nanofabricated substrate, unfortunately, is limited by its fabrication difficulty under the nano-scale, such as less than 10 nm [2]. Therefore, the development of new approaches to prepare the SERS substrate receives increasing attention around the world [5, 6].

For example, an ordered two-dimensional or three-dimensional silver (Ag) NP assembly was obtained with the help of a nanostructured template [7, 8]. An alternative template is a porous matrix, such as porous alumina [9] and porous semiconductors [10, 11]. For example, an Ag-coated silicon (Si) nanopore was tested as a SERS substrate after thermal decomposition of silver nitrate ($AgNO_3$) salt that had been adsorbed onto the pore wall [12]. Sailor *et al* prepared a SERS substrate from an Ag-plated porous Si. Due to the electroless redox reaction between the oxidation of porous Si and the reduction of Ag^+, an Ag NP assembly, and even Ag dendrites, were deposited onto the porous template [4].

Sailor's approach, however, needs three steps to get a SERS substrate, including the first nucleation process, subsequent etching to obtain the porous Si, and an Ag NP deposition (by an electroless redox reaction) to finally yield the SERS substrate [4]. Regarding the electroless redox reaction,

the oxidation of Si, no matter whether it occurs on a flat Si wafer or on a porous template, provides the driving force for the reduction of Ag^+. The reduction product can be deposited on the Si surface and works as the metal nucleus for the pore-etching reaction [13]. Therefore, the nucleation and the etching processes are able to be merged into the Ag NP deposition. In this report, this assumption of one step to get a SERS substrate was tested by dipping a flat Si wafer into an aqueous deposition solution of hydrogen fluoride (HF) + $AgNO_3$ [13, 14]. HF is introduced to keep the electroless redox reaction sustainable because it can dissolve and remove Si oxide. Otherwise, the Si oxide can be re-formed by the oxidation reaction occurring on the bare Si surface and thus cover the surface, even where the oxide has previously been removed. Since the Si oxide is insulative, it can barricade the redox reaction by stopping the oxidation of Si or by blocking the transport of electrons from the oxidation frontier to the reduction frontier. The former takes place on the bare Si surface, whereas the latter takes place on the metal nucleus surface. Furthermore, in the presence of HF, the growth of Ag NPs means the development of the porous Si [10], which can consequently accelerate the growth of Ag NPs by increasing the surface area of the oxidation reaction. Therefore, on the one hand, the original surface is not a bumpy porous Si but a flat Si wafer, on which a uniform layer of NPs can be deposited. On the other hand, the subsequently resulting porous Si offers the needed high reactivity for the preparation of an Ag NP assembly with a high coverage by self-driving and accelerating the deposition process. This one-step approach holds the promise to prepare a SERS substrate at the point-of-use for the field application.

The sample-loading method onto the SERS substrate was also studied, (i) by incubating the as-prepared substrate in the sample solution, (ii) by dropping and drying a small volume of sample solution onto the substrate surface, or (iii) by directly introducing the sample into the deposition solution. The last method has further simplified the operation because the SERS substrate's preparation and its sample loading were simultaneously conducted. This method was also applied to metalize a Si nanowire (NW) [15–17]. In terms of the large specific surface area to grow Ag NPs, the highly curved Si NW surface is comparable with the porous Si. Furthermore, compared to the porous structure where the deposition reaction occurs, an isolated and regular NW array can improve the transport efficiency of reactants and products to or from the reaction frontier. That is because the reaction frontier is focused onto the Si NW surface which has been exposed to the deposition solution, unlike the situation for the pore structure where the deposition solution is trapped inside the pore. The NW's mini surface concentrated all the deposited Ag NPs and forced them to self-assemble along the NW with a uniform distribution and a high reproducibility. The aggregated Ag NPs also exhibited a high enhancement for the Raman scattering.

2. Materials and methods

2.1. Reagents and materials

Rhodamine 6G (R6G), nucleic acid bases adenine (A), thymine (T), cytosine (C), and guanine (G) and other reagents were purchased from Sigma-Aldrich. Ag^+ solution was prepared with deionized water and stored at 4 °C in the dark. *HF must be carefully handled and a mask is always necessary.*

2.2. Preparation of SERS substrate

A Si wafer with a size of 1 cm × 2 cm was used as a flat template and its surface orientation was {100}. In this report, there was no obvious influence from the doping level and doping type (n- or p-type). The surface oxide was removed by dipping the wafer into ammonium fluoride etchant (Merck, TB 1063) for ∼1 min. After being washed with deionized water, the wafer was immediately used for the Ag NP deposition.

The Si wafer was dipped into an aqueous deposition solution of 5 M HF + 10 mM $AgNO_3$ or others for various periods of time in the dark. After being washed with deionized water and 70% ethanol, the metalized Si wafer surface could be used as a SERS substrate. Scanning electron microscopy (SEM, JSM-6700F, Japan) was employed for physical characterization of the SERS substrate.

All Si NW arrays were fabricated at the Institute of Microelectronics, Singapore [18]. Due to its pattern fabrication process, lithography and oxidation, the bottom bed of the resulting Si NW is a thick layer (∼150 nm) of Si oxide. The preparation of the SERS substrate was kept the same as above.

2.3. Loading of sample

The to-be-detected sample was R6G or nucleic acid bases A, T, C and G. Three methods were individually employed to load the sample species onto the SERS substrate.

First, the as-prepared substrate was incubated in an aqueous solution containing the sample for ∼3 h in the presence of 1 mM NaCl [19]. The substrate was then washed with deionized water and dried with nitrogen. The substrate with the sample loaded was then stored in the dark in a sealed box for the later measurement. It was found that it could be kept stable for at least 24 h.

Second, a small volume of the sample solution, about 1–2 μl, was dropped onto the as-prepared substrate surface. Then the substrate was put into an oven at a temperature of 37 °C and dried within 10 min. After that, it can be used for SERS testing.

Third, the sample can be loaded by directly introducing the sample into the deposition solution mentioned in section 2.2. Following the same preparation procedure, the resulting Si wafer was washed with deionized water, 70% ethanol and dried carefully with nitrogen. The washing step can even be skipped, as discussed in the following.

2.4. Raman microscopy

All SERS spectra were collected at room temperature (∼24 °C) in air with the help of a Renishaw 2000 Raman microscope equipped with a near infrared 785 nm diode laser (24 mW). The laser beam was set in position through a Leica Imaging Microscope objective lens (50×). A CCD detector was used to collect the Stokes Raman signal in a wavenumber range of 600–2000 cm^{-1} for an exposure time slot of 10 s. At least three spectra were independently recorded from the random

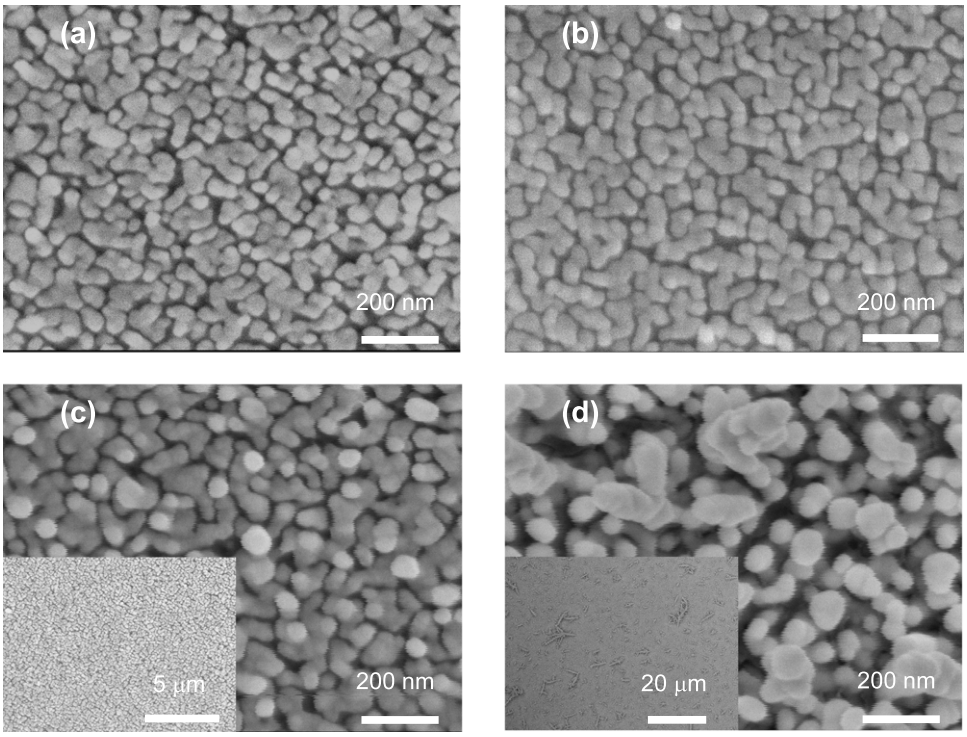

Figure 1. SEM pictures of the as-prepared SERS substrates. The preparation was carried out by dipping a flat Si wafer into a deposition solution of 5 M HF + 10 mM $AgNO_3$ for (a) 5 s, (b) 10 s, (c) 20 s and (d) 60 s, respectively.

position on each substrate surface in an attempt to characterize the possible non-uniform distribution. The spectrum curve has been shifted off-scale but without being corrected to get a clear curve array for comparison.

3. Results and discussion

3.1. Substrate preparation from a flat Si wafer in the absence of sample

Morphology. In figure 1, the Ag NP assemblies are observed by the one-step dipping approach. The size of the individual NPs is dependent on the dipping time. The longer it is, the larger the NP is, with a diameter from ∼30 nm for 5 s in figure 1(a) to ∼50 nm for 10 s in figure 1(b), to ∼80 nm for 20 s in figure 1(c), respectively. The deposition reaction behaved so fast that a monolayer of NPs was obtained within ∼20 s. One reason is that the Si wafer is a reductant reagent, another is that the developed porous Si can accelerate the self-driving deposition reaction due to the increased surface area for the oxidation reaction to take place [4, 20]. A too long dipping time, such as 60 s, however, leads to a non-uniform distribution. Not only is the attachment of the neighboring NPs observed, but also the multilayer and the Ag dendrites come into sight in figure 1(d).

In figure 2, the porous structure is observed after lifting-off the Ag NP layer, evidencing the assumption of the one-step preparation mechanism [10]. Compared to the bumpy template of a deeply-etched porous Si [4], the shallow pores on a flat surface can generate a uniform distribution of the Ag NP assembly, as presented in figure 1(c). In figure 2(b), Ag dendrites appear on the edge of the Si wafer. Therefore, the transport of the reactants or products to or from the different reaction frontiers is critical for the preparation of a uniform substrate, which will be further discussed in the following.

The deposition of metal onto the semiconductor surface has been studied for theoretical understanding and for application [20]. As a simplified version without an external net current, the electroless deposition process receives increasing attention [13, 14]. The deposition of Ag NPs by reducing Ag^+ involves either electron extraction from the semiconductor's conduction band or hole-injection into its valence band; one of these approaches provides the driving force for the reduction reaction, or vice versa. As for the Ag NPs deposited on the Si wafer, there is no significant effect from the doping level and type. That is, the oxidation of Si involving electrons, not holes, should dominate the electroless redox process [10]. As a consequence, HF should be introduced into the deposition solution to dissolve the insulative oxide layer and to keep the deposition reaction sustainable, as shown in the following [13, 14].

$$Ag^+ + e = Ag \tag{1}$$

$$Si + 2H_2O = SiO_2 + 4H^+ + 4e \tag{2}$$

$$SiO_2 + 6HF = H_2SiF_6 + 2H_2O. \tag{3}$$

In total,

$$Si + 4Ag^+ + 6HF = H_2SiF_6 + 4H^+ + 4Ag. \tag{4}$$

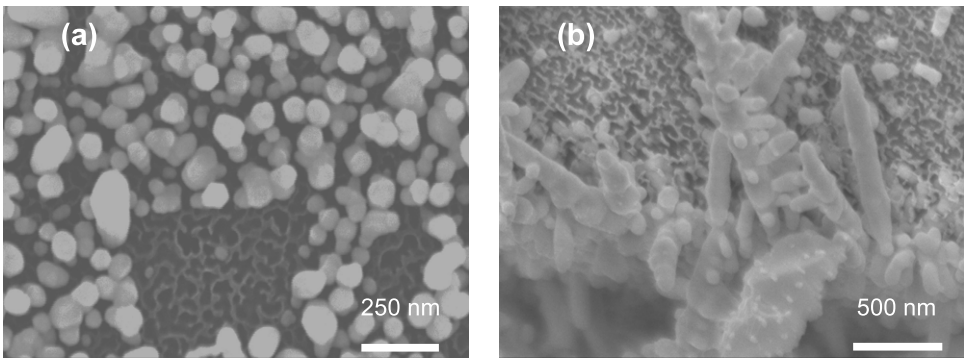

Figure 2. SEM pictures of the porous structure developed on the bottom Si wafer after lifting-off the Ag NP layer. The dipping time was 60 s and the rest was kept the same as in figure 1. (a) Central part; (b) edge of the Si wafer.

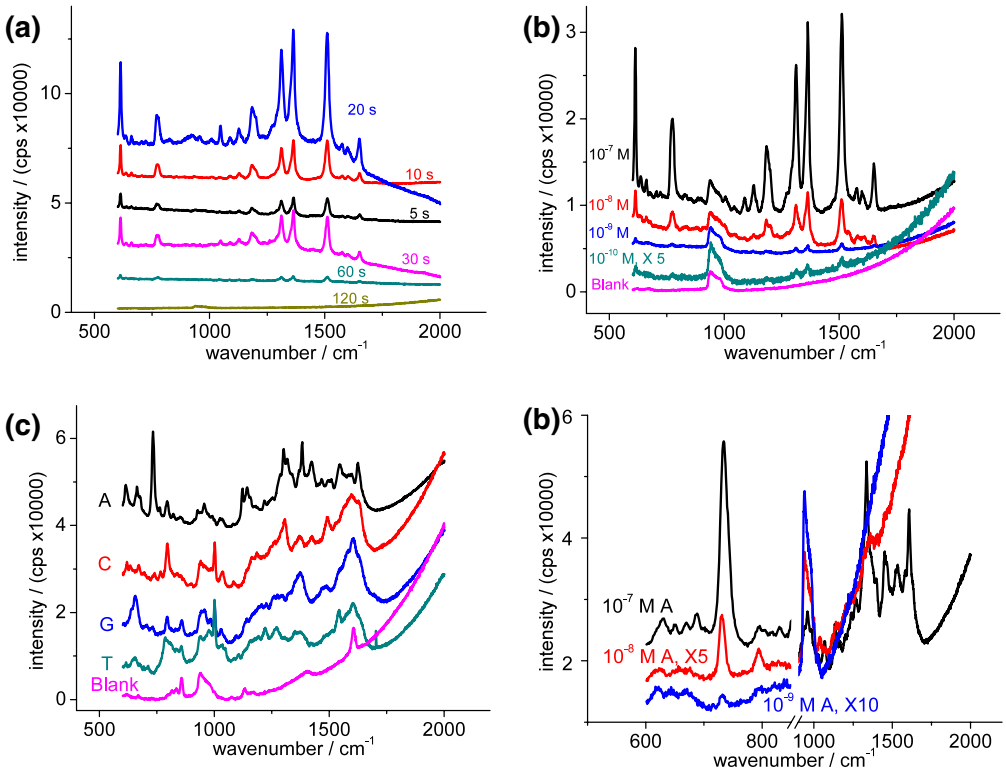

Figure 3. SERS spectra collected from the SERS substrates presented in figure 1. The effect of the dipping time can be seen in (a). For (b)–(d), the dipping time was fixed at 20 s. The sample of R6G in (a), (b) was different from the nucleic acid base in ((c), (d)). The sample-loading method was also different, either by incubating the as-prepared substrate in ∼5 ml sample solution for 3 h in the presence of 1 mM NaCl (a), (b) or by dropping 1–2 μl of sample solution onto the substrate surface and drying at 37 °C within 10 min (c), (d). The sample's concentration was 1×10^{-7} M (a), (c) or as indicated in the curves (b), (d).

SERS response. The Ag NP assemblies in figure 1 have been tested as SERS substrates and the results are listed in figure 3. In figure 3(a), the variation of the dipping time exhibits an influence on the intensity of the Raman signal. With the prolonging of the dipping time, the Raman signal was strengthened and reached its maximum at about 20 s, which was due to the shortened interdistance among the neighboring NPs, as shown in figure 1(c). After that, the further prolonged dipping time led to a declined intensity, suggesting a weakened enhancement owing to the attachment among the neighboring NPs, as shown in figure 1(d) [2]. Therefore, a dipping time of 20 s was selected to prepare the SERS substrate for the following experiments. Using the optimized substrate, a limit of detection of $\sim 1 \times 10^{-10}$ M R6G can be reached by incubating the substrate in the sample solution, as presented in figure 3(b). The enhancement factor is $\sim 10^6$ when compared to the signal obtained from a flat surface.

During the long incubation period (∼3 h), lift-off of the Ag NP layer from the substrate surface was usually observed, as shown in figure 2. In an effort to avoid this, a small volume of the sample solution (1–2 μl) was directly dropped onto the substrate surface and dried. The collected spectra are listed in figure 3(c). Herewith the DNA bases of A, T, C and G were used as the Raman scatterers to test the bio-application of the as-prepared SERS substrate [1, 21]. The characteristic peaks are identified at 733, 1323, 1454 cm^{-1} for A; 795, 1305, 1596 cm^{-1} for C; 654, 1375, 1605 cm^{-1} for G and 787, 1605 cm^{-1} for T, respectively.

The interference peaks in the region of 900–1100 cm^{-1} and the fluorescence background in the region of 1100–1700 cm^{-1} should originate from the porous Si [22] or from the Si–Ag composite [23]. In figure 3(c), there are also several other interference peaks from the blank substrate, which overlap onto the Raman signal from the target sample. Perhaps those peaks originate from the adsorbed F^- on the Ag NP surface [24, 25]. Fortunately, those peaks were weakened with the prolonging of the dipping time from 5 to 120 s (not shown here). Perhaps the expanded NPs brought about a decreased specific surface area and a low capacity to load F^- [2, 26]. On the other hand, the blank substrate's interference was negligible when the incubation method was employed to load sample species, as shown in figure 3(b). The long incubation time (∼3 h) can lead to the exchange of the adsorbed F^- on the Ag NP surface with the sample species or Cl^- from the incubation solution.

In figure 3(d), the as-prepared SERS substrate is tested by dropping and drying a low concentration of base A on the substrate surface. Regarding its characteristic peak of 733 cm^{-1} [27], a detection limit of $\sim 1 \times 10^{-9}$ M is reached, which is comparable to $\sim 1 \times 10^{-10}$ M R6G in figure 3(b). If ignoring the difference in the sample molecule itself, a possible reason for the difference is due to the different orientation of the sample molecule on the substrate, which is relative to the sample-loading method. During the long incubation period, the sample molecules can rotate and locate onto the substrate surface with a preferable orientation. The preferable molecular orientation on the surface can boost the chemical enhancement. In other words, in figures 3(b) and (d), the electromagnetic contribution should be the same because the substrate surface nanostructure is the same. Therefore, the difference mainly originates from the chemical contribution [1, 2]. That is, the long sample-loading time is preferable not only to get a clean background (less interference from F^-), but also to obtain an improved molecular orientation. For field application, however, the testing speed and operation simplification are highly desirable so that there must be a balance between the loading time and the detection limit.

3.2. Substrate preparation from a flat Si wafer in the presence of sample

Morphology. The sample was loaded either by incubating the as-prepared SERS substrate in the sample solution for 3 h or just by dropping the sample solution onto the substrate surface and drying within 10 min, as mentioned above [4, 19]. Due to the one-step preparation of the SERS substrate, the sample can also be directly loaded from the Ag NP deposition process. That is, the deposition solution of HF + $AgNO_3$ was replaced with HF + $AgNO_3$+ sample, which could further simplify the operation procedure and shorten the operation time for the field application. To simplify the experiment, only R6G is selected as the sample for the following testing because there is a complicated coordination interaction between Ag^+ and DNA bases. The obtained nanostructures and Raman spectra are listed in figures 4 and 5, respectively.

In the hope of diminishing the interference from the adsorbed F^-, a deposition solution of a low concentration of HF should be selected [24, 25]. On the other hand, in order to keep the deposition reaction sustainable, there should be free HF species after coordinating with Ag^+. In this report, the concentration ratio between HF and $AgNO_3$ was kept at 10:1 or more. In the presence of 1×10^{-6} M R6G, the varied concentration of the deposition component of HF + $AgNO_3$ brings about the different morphology of the deposited NP assembly, as shown in figure 4.

In figure 4(a), a larger size of individual Ag NPs with a poorer uniformity than that in figure 1(c) is observed, although both have experienced the same dipping time and the same concentration of $AgNO_3$. As the concentration of HF was diluted from 5 to 1 M, the nucleation process was barricaded in turn and the driving force for the deposition reaction shifted [13]. Another possible reason includes the introduction of R6G into the deposition solution.

In figure 4(b), when the concentration of $AgNO_3$ is decreased, small NPs are obtained, indicating a decelerated growth kinetics for the individual NPs [28]. With the prolonging of the dipping time, each Ag NP grows homogeneously, as presented in figure 4(c). A NP assembly with a uniform distribution can be seen from the inset picture, suggesting the transport of reactants or products is uniform under this condition.

The further dilution of the deposition component led to a slower reaction, even 10 min was needed to get an obvious NP assembly, as listed in figure 4(d). Its distribution is not uniform and its size is not unique owing to the inhomogeneous growth, which are mainly due to the random nucleation and the non-uniform transport to the random nucleus in the diluted solution [28].

SERS response. As the sample has been simultaneously loaded during the substrate's preparation process, the Raman signal can be promptly collected, which is suitable for the field application. The Ag NP assembly in figure 4(a) yields the spectra in figure 5(a). For comparison, a standard spectrum of R6G is also listed. The characteristic peaks of R6G can be identified from the background. The uniform distribution of the NP assembly is evidenced from the similar spectrum array collected from the different position on the substrate.

When the deposition component of HF + $AgNO_3$ was diluted, the Raman intensity was strengthened (figure 5(b)) with the growth of the individual NPs from figures 4(b) to (c). As for the dipping time of 60 s, the uniformity of the Ag NP

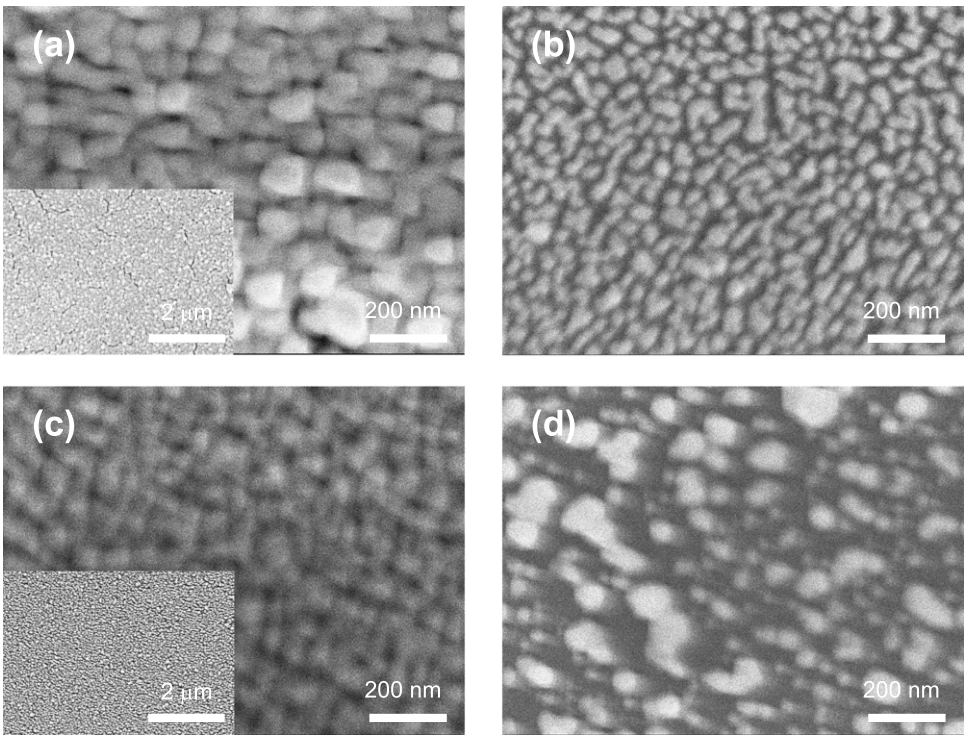

Figure 4. SEM pictures of the deposited Ag NP assembly on a flat Si surface. In the presence of 1×10^{-6} M R6G, the deposition was carried out in 1 M HF + 10 mM $AgNO_3$ for 20 s (a), 10 mM HF + 1 mM $AgNO_3$ for 20 s (b) or 60 s (c), 1 mM HF + 0.1 mM $AgNO_3$ for 10 min (d), respectively.

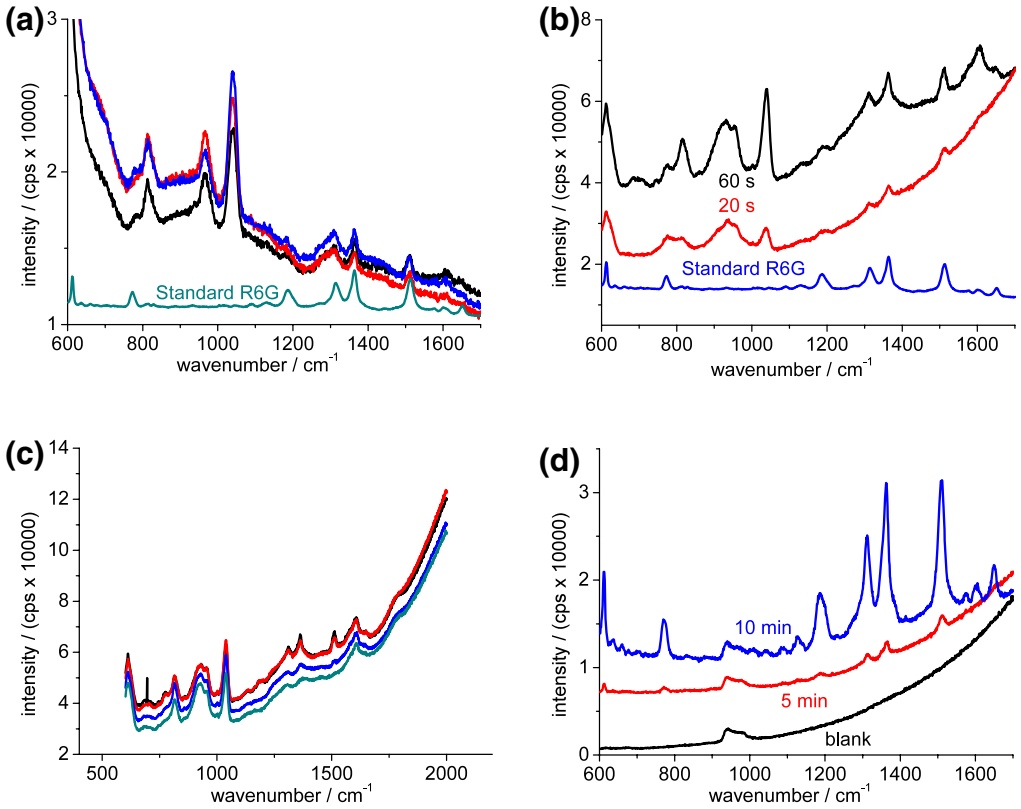

Figure 5. SERS spectra collected from the Ag NP assemblies presented in figure 4. (a) is collected from the assembly shown in figure 4(a), (b) from figures 4(b) and (c), (c) from figure 4(c) and (d) from figure 4(d), respectively.

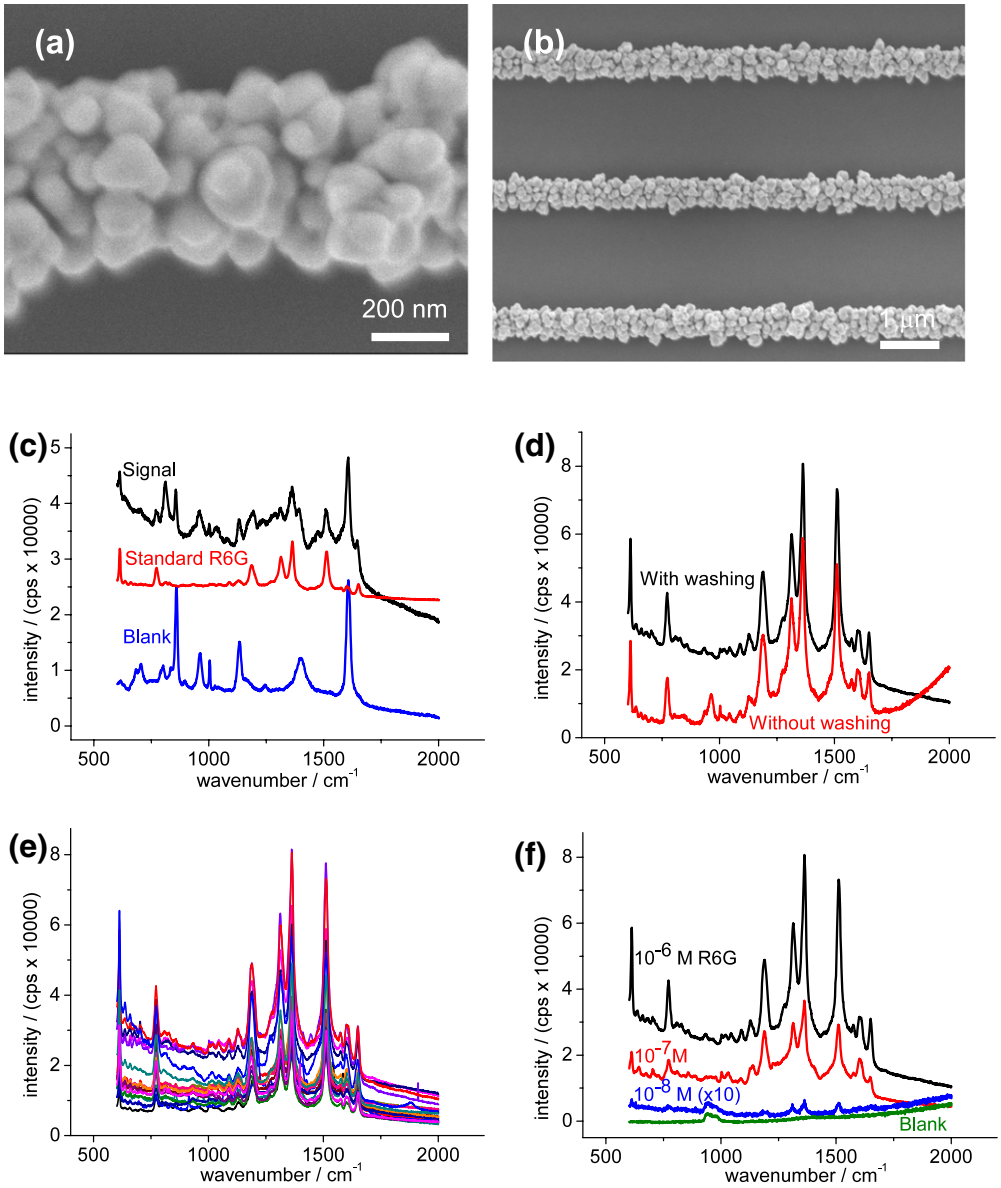

Figure 6. (a), (b) SEM pictures and (c)–(f) SERS spectra. The metalization was carried out by dipping the NW array into a solution of 1 mM HF + 0.1 mM $AgNO_3$ + 1 × 10^{-6} M of R6G. The dipping time was 5 min except (c) 1 min. The effect of the washing step after the sample preparation is shown in (d). The reproducibility of the as-prepared substrate can be seen from the spectra collected from three different metalized NW arrays, as shown in (e). The limit of detection can be seen in (f) when the concentration of R6G is varied.

assembly can be seen from the similar spectrum array listed in figure 5(c). Although the improvement is observed when compared to figure 5(a), the background is still significant. By further prolonging the dipping time, however, the Ag NPs grow into a non-uniform NP assembly, even into a dendrite or a bulk film. The corresponding Raman signal is also weak (not shown here).

The R6G's Raman scattering signal is clearly identified in figure 5(d), particularly for a dipping time of 10 min, evidencing the assumption of the advantage of a long sample-loading time. However, the distribution of the resulting NP assembly is not uniform, as observed in figure 4(d). Even so, it demonstrates the capability to directly load the sample onto the substrate from the Ag NP deposition process.

3.3. Substrate preparation from a Si NW in the presence of sample

In figure 4(d), the nucleation occurs at random on the flat Si surface. In order to get a uniform SERS substrate, a Si NW is used as a deposition template in order to concentrate all the deposited Ag NPs onto the NW's mini surface [15–17]. As only the Si NW surface works as the reaction frontier after being exposed to the deposition solution, the transport of reactants and products can be improved from the plane diffusion near a flat Si wafer to the semi-cylinder diffusion surrounding a NW. The resulting nanostructure is shown in figures 6(a) and (b). Only the Si NW is covered with the Ag NPs under the background of Si oxide, evidencing the above assumption. The larger NP in figure 6(a) compared

with that in figure 4(d) should originate from the improved transport.

The resulting substrate can also be directly used for Raman signal collection. As for the dipping time of 1 min, the obtained signal in figure 6(c) ('signal') seems to be a matrix spectrum from R6G and from F^-. When a control experiment was carried out in the absence of sample in the deposition solution, the strong signal from the adsorbed F^- ('blank') was observed, implying the enhancement from the Ag NP assembly aggregated along the NW. The spectrum of R6G is also listed for comparison. The characteristic peaks of R6G can be identified, suggesting the success of using the metalized Si NW as a SERS substrate.

When the dipping time was 5 or 10 min, the sample signal was strengthened and the background weakened (figure 6(d)). Perhaps the highly curved NW surface can prevent the neighboring NPs from attaching into a bulk metal film. As a consequence, there is a high electric–magnetic field among the neighboring NPs that individually aggregated on the NW. When the sample molecule was loaded and trapped in this high electric-magnetic field, the Raman signal with a high enhancement was observed [15–17]. Even the washing step after the deposition, which is supposed to remove the physically adsorbed species, cannot bring a significant improvement, indicating a clean SERS substrate was prepared from the deposition solution of HF + $AgNO_3$ + sample. The reproducibility of the substrate is challenged by putting together 18 curves collected from three different NW arrays (figure 6(e)). The similar spectra indicate a uniform Ag NP assembly distributed on the NW array.

Finally, the Ag NP was deposited in the presence of various concentrations of R6G. A low concentration of $\sim 1 \times 10^{-8}$ M R6G can be detected, as presented in figure 6(f). Compared to the detection limit of $\sim 1 \times 10^{-10}$ M R6G in figure 3(b) and $\sim 1 \times 10^{-9}$ M A in figure 3(d), the simplified operation in figures 4–6 is preferable for the field application. There is no additional sample-loading step, although its limit of detection is not as low as the others. On the other hand, when compared to the Raman scattering signal obtained from the flat Si oxide surface, the enhancement factor is estimated to be $\sim 10^6$ in figure 3(b), $\sim 10^5$ in figure 3(d) and $\sim 10^6$ in figure 6(f), respectively. As discussed above, the larger value in figure 3(b) compared with that in figure 3(d) is likely due to the chemical contribution stemming from the incubation process in the presence of NaCl. However, a similar value, even a higher one in figure 6(f) than that in figure 3(b), originates from the aggregated NPs along the highly curved surface of the Si NW, which can be further improved due to its three-dimensional structure.

4. Conclusions

A simple approach has been developed to prepare the SERS substrate just by dipping a Si wafer into an aqueous deposition solution. Within minutes, a monolayer of Ag NP was uniformly deposited on the flat Si surface. When used as a SERS substrate, it exhibited a high enhancement.

The sample-loading method was challenged by directly introducing the sample into the deposition solution. The simplified approach was also employed to metalize the Si NW. Due to the highly curved and mini surface, all the Ag NPs self-assembled along the NW and aggregated into an efficient SERS substrate with a high reproducibility. The simple and quick approach holds promise for the field application because a clean and fresh, oxide-free SERS substrate can be prepared at the point-of-use and the sample can be simultaneously loaded for a prompt Raman scattering collection.

As the deposition of the Ag NP onto the NW surface only consumed a small volume of the deposition solution whereas ~5 ml of solution was used to prepare the SERS substrate by the dipping approach, perhaps a small volume of the deposition solution of HF + $AgNO_3$ + sample can also be dropped onto the NW array to get a SERS substrate with the sample loaded. The preliminary result is exciting and further experiments are ongoing.

Acknowledgments

The fruitful discussion and the instrument support from Effendi Widjaja, Marc V Garland, Nizamudin Mohamed Khalid, and Shaik Mohamed Salim are greatly appreciated.

References

[1] Kneipp K, Kneipp H, Itzkan I, Dasari R R and Feld M S 1999 *Chem. Rev.* **99** 2957–75
[2] Haynes C L, McFarland A D and Duyne R P V 2005 *Anal. Chem.* **77** 338A–46A
[3] Nie S and Emory S R 1997 *Science* **275** 1102–6
[4] Lin H, Mock J, Smith D, Gao T and Sailor M J 2004 *J. Phys. Chem.* B **108** 11654–9
[5] Deng S, Fan H M, Zhang X, Loh P K, Cheng C-L, Sow C H and Foo Y L 2009 *Nanotechnology* **20** 175705
[6] Zhai J, Wang Y, Zhai Y and Dong S 2009 *Nanotechnology* **20** 055609
[7] Song W, Li W, Cheng Y, Jia H, Zhao G, Zhou Y, Yang B, Xu W, Tian W and Zhao B 2006 *J. Raman Spectrosc.* **37** 755–61
[8] Kalkan A K and Fonash S J 2005 *J. Phys. Chem.* B **109** 20779–85
[9] Kuncicky D M, Prevo B G and Velev O D 2006 *J. Mater. Chem.* **16** 1207–11
[10] Föll H, Carstensen J, Christophersen M and Hasse G 2000 *Phys. Status Solidi* a **182** 7–16
[11] Fang C, Föll H and Carstensen J 2006 *J. Electroanal. Chem.* **589** 259–88
[12] Chan S, Kwon S, Koo T-W, Lee L P and Berlin A A 2003 *Adv. Mater.* **15** 1595–8
[13] Peng K, Hu J, Yan Y, Wu Y, Fang H, Xu Y, Lee S and Zhu J 2006 *Adv. Funct. Mater.* **16** 387–94
[14] Garnett E C and Yang P 2008 *J. Am. Chem. Soc.* **130** 9224–5
[15] Leng W, Yasseri A A, Sharma S, Li Z, Woo H Y, Vak D, Bazan G C and Kelley A M 2006 *Anal. Chem.* **78** 6279–82
[16] Yasseri A A, Sharma S, Kamins T I, Li Z and Williams R S 2006 *Appl. Phys.* A **82** 659–64
[17] Li C-P, Wang N, Wong S P, Lee C-S and Lee S-T 2002 *Adv. Mater.* **14** 218–21

[18] Gao Z, Agarwal A, Trigg A D, Singh N, Fang C, Tung C-H, Fan Y, Buddharaju K D and Kong J 2007 *Anal. Chem.* **79** 3291–7
[19] Fang C, Agarwal A, Buddharaju K D, Khalid N M, Salim S M, Widjaja E, Garland M V, Balasubramanian N and Kwong D-L 2008 *Biosens. Bioelectron.* **24** 216–21
[20] Zhang X G 2001 *Electrochemistry of Silicon and its Oxide* (New York: Kluwer Academic–Plenum)
[21] Rasmussen A and Deckert V 2006 *J. Raman Spectrosc.* **37** 311–7
[22] Canham L T 1990 *Appl. Phys. Lett.* **57** 1046–8
[23] Lu Y W, Du X W, Sun J, Han X and Kulinich S A 2006 *J. Appl. Phys.* **100** 063512
[24] Kwok W M, Gould I, Ma C, Puranik M, Umapathy S, Matousek P, Parker A W, Phillips D, Toner W T and Towrie M 2001 *Phys. Chem. Chem. Phys.* **12** 2424–32
[25] Schmitt E W, Huffman J C and Zaleski J M 2001 *Chem. Commun.* **2** 167–8
[26] Le F, Brandl D W, Urzhumov Y A, Wang H, Kundu J, Halas N J, Aizpurua J and Nordlander P 2008 *ACS Nano* **2** 707–18
[27] Domke K F, Zhang D and Pettinger B 2007 *J. Am. Chem. Soc.* **129** 6708–9
[28] Simm A O, Ji X, Banks C E, Hyde M E and Compton R G 2006 *ChemPhysChem* **7** 704–9